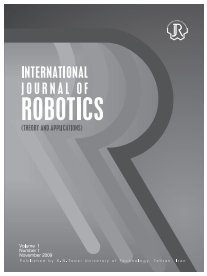

INTERNATIONAL JOURNAL OF ROBOTICS
(THEORY AND APPLICATIONS)
E-mail: IJR@kntu.ac.ir

Optimal Design of Dexterous Cable Driven Parallel Manipulators

Mohammad M. Aref[a], Hamid D. Taghirad[a] and Sasan Barissi[b*]

a- Advanced Robotics and Automated Systems (ARAS), Faculty of Electrical and Computer Engineering, K.N. Toosi University of Technology, Tehran, Iran.
b- Engineering Department, Purdue University Calumet, Hammond, IN, US, sbarissi@calumet.purdue.edu .

ARTICLE INFO

Article history:
Received: July 10, 2009
Received in revised form:
November 11, 2009
Accepted: December 2, 2009

Keywords:
Cable Driven Parallel Manipulators
Redundant Mechanisms
Multi Objective Optimal Design
Cost Function Definition

ABSTRACT

Optimal design of parallel manipulators is known as a challenging problem especially for cable driven robots. In this paper, optimal design of cable driven redundant parallel manipulators (CDRPM) is studied in detail. Visual Inspection method is proposed as a systematic design process of the manipulator. A brief review of various design criteria shows that the optimal design of a CDRPM cannot be performed based on single objective. Therefore, a multi objective optimal design problem is formulated in this paper through an overall cost function. Furthermore, a proper weighting selection for the overall cost function is proposed, which can be viewed as a promising method to the open problem of parallel manipulator design. In order to verify the effectiveness of the proposed method, it is applied on the design of KNTU CDRPM, an eight actuated with six degrees of freedom CDRPM, which is under investigation for possible high speed and wide workspace applications in K. N. Toosi University of Technology. Finally, a combined numerical optimization algorithm is used to find the unique global optimum point. The result shows a significant enhancement in the performance characteristics of the KNTU CDRPM compared to that of the other CDRPMs. Since the proposed method is not restricted to any particular assumption on the objectives and design parameters, it can be used for optimal design of other manipulators.

1. Introduction

Increasing demand for high acceleration and energy efficient manipulators in a wide workspace necessitates determining an optimal design solution in accordance with restrained resources. An optimal design solution is a set of design parameters which satisfies the objectives defined by a particular optimality criterion. The complexity of structure and multitude of parameters, constraints, and optimality objectives make the optimal design procedure complex for serial and much more extensive for *Parallel Manipulator*s (PM) [1]. Various methods have been used in optimal design of serial and PMs. Analytical synthesis methods are very complex and even impossible to be performed for the real serial or PM designs with more than 3 *degrees-of-freedom* (DOF). As an alternative, defining an optimality index and trying to force the design parameters to minimize this index is another common approach [2, 3]. Although it is shown in the literature that these indices work impeccably well for a specific structure, however, they are usually not applicable to a general class of robotic structures due to their scale dependence [4], and moreover, different optimality measures have been introduced and compared in the literature [4, 5]. In spite of the fact that these mathematical methods cannot provide a transparent view of dependency of the parameters the optimality region and its convexity, some graphical tools are used in order to make the

*** Address for correspondence: sbarissi@calumet.purdue.edu**

visualization more clear. As an example, [6], show dependency of optimality criterion on different poses in a graph by ellipsoids for serial robots and [7] illustrate that for cable-driven PMs.

Although optimal design methods can be useful to improve efficiency and other required objectives, they cannot improve characteristic deficiencies caused by kinematic structure. For instance, a task like flight simulator which demands high safety, accuracy, acceleration, and stiffness cannot be implemented by a serial manipulator. Nowadays, PMs meet all of these demands [8] as well as high payload to moving mass ratio. On the other hand, using massive stroke-limited hydraulic or pneumatic actuators in a parallel mechanism [9] results in their limited workspace and existence of several singular points within the workspace [10]. Thus, using electrically powered cable–driven actuators instead of rigid linear actuators significantly reduces the physical limitations on workspace boundaries and the complexity of manufacturing. By this means, a *Cable–Driven Redundant Parallel Manipulator* (CDRPM) can be designed such that whose workspace is as large as a football stadium [11], or to the extent of the platform of a large adaptive reflector with square kilometer footprint [12]. Furthermore, CDRPM saves heredity of PMs on acceleration capabilities at the cost of its control complexity. Besides, cables can only carry axial tension forces and they are unable to bear any compression or bending. Therefore, tension force feasible workspace is another important aspect of CDRPMs [13]. Conceptual designs of such manipulators lead to find the end–effector in a workspace surrounded by the cables. Thus, design procedure of CDRPMs not only necessitates satisfying dexterity measures, but also requires force feasible and collision free workspace. On the other hand, redundancy is necessary to have force feasible workspace which increases the number of design parameters and complexity of optimal design procedures. Therefore, a multi objective design method must be proposed to fulfill all of the objectives in an optimal design.

Although many researches are conducted on optimal design of manipulators, there are few comprehensive studies in the field of CDRPMs [7, 14, 15]; even those are solely focused on the tension force feasible workspace. In this paper by using a special structure of KNTU CDRPM, geometrical workspace of CDRPMs is studied in detail by focusing the optimal design procedures. In the most of the reported research results only force feasibility in the workspace is analyzed, and through this analysis the boundaries of the cable driven robot workspace is determined [16]. In those cases the analysis of self collisions is ignored, since such possibility is diminished by the robot design structure. Nevertheless, this is accomplished by enforcing stringent boundaries into the force feasible workspace. However, in this paper a totally different approach is proposed to design the KNTU CDRPM based on collision avoidance scheme, force feasibility, and dexterity, simultaneously. Weighting of cost functions are known as the main problem in multi objective optimal design of PM as described in [1]. This problem is solved by the proposed weighting functions for each cost according to the illustrated graphs by means of formulating qualitative design objectives. As a result, a significant change in the structure of the KNTU CDRPM is obtained compared to that of the other reported designs.

Accordingly, a method is needed to determine parameters role and their dependency, verify convexity of the optimal region, and finally solve the multi objective design problem. To consider all these issues simultaneously and being able to reach to a solution, a visual inspection method is proposed which is suitable for optimal design of complex manipulators such as a CDRPM. In this method dependency of the parameters and the convexity of objective functions are easily illustrated. Additionally, analysis of the given graphs facilitates to select effective design parameters, propose appropriate weights and costs for objectives, verify optimal region, and encapsulate some physical objectives into the design procedure. By this means, a numerical optimization tool becomes capable of converging to a unique optimum design point without being stuck in an unwanted local minimum.

In this paper, *Visual Inspection* (VI) method is elaborated in detail which includes steps to show potential dependency of parameters and definition of a boundary containing the optimal point. Then, a method is recommended to extract cost functions of different objectives from the graphs. To implement the method, the *KNTU CDRPM* is introduced. The KNTU CDRPM is designed based on a structure with eight actuators and six degrees of freedom. This manipulator is under investigation for possible high speed and wide workspace applications such as tool manipulation in K. N. Toosi University of Technology. Next, the VI method is implemented on the optimal design of KNTU CDRPM. Finally, different numerical optimization algorithms are used to find the unique global optimum point. The result shows a significant enhancement in the performance characteristics of the KNTU CDRPM compared to that of the other CDRPMs [9].

2. Visual Inspection Method

2-1. Graph Generation

In an optimal design procedure a primary conceptual design is selected with some simplified design parameters which are optimized with respect to some objective functions. This simplification reduces the optimization complexity, and computation cost and increases the chance to achieve an optimal solution. Noticing the fact that some of the parameters are independent from the objective function, these parameters can be excluded by the proposed VI method.

Assume that a_i, i=1,…,p are primary conceptual design parameters in which p is the number of design parameters. These design parameters have to be optimized with respect to the following objective functions: C_i, i=1,…,q. First, the graph of an objective function, like C_i, for different values of a_i, a_j is plotted in a way that the color of each point represents the value of the objective function as shown in figure 1. According to the graph, if there is not an obvious change in color of the graph, the objective function is independent of the chosen parameters. In this case, other objectives must be tested; if an objective is independent of all parameters, the objective is not useful or the parameters are not sufficient. In other words, gradient of the color scheme is sensible to the role of the design parameters in each objective function. The graph of an objective function can be categorized into similar graph patterns shown in figures 1, 2, 3, and 4. In figure 1 the objective function converges to an optimum solution considering two parameters. This result is convex which is desirable to find an optimal solution.

In figure 2 two possible incidents can be predicted; the range of a_j parameter is chosen inappropriately. Otherwise the optimum result is achieved when the parameter converges to infinity. In other words, the objective function is scale dependent, and therefore, this parameter is limited to some practical constraints. If this condition applies to both of the parameters, the result is similar to figure 3. If the graph pattern is similar to figure 4, the objective function is independent of the parameter represented by a_i. If the graph pattern is similar to figure 4, it is recommended to use the ratio of these design parameters in the optimization, since their role in the objective function is strongly related to each other. Finally, if the above conditions do not apply and the graph does not have any regular shaped pattern, the graph must be restructured to find a regular pattern. For example, the ratio of parameters can be studied, or the grid resolution can be increased in the numerical search algorithms.

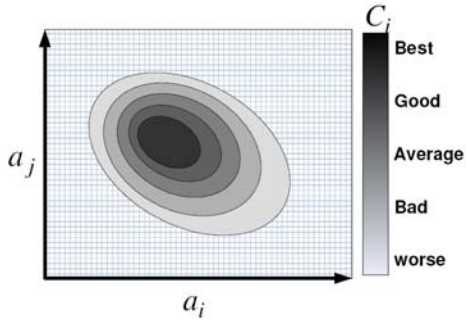

Figure 1: A convex graph for a pair of parameters

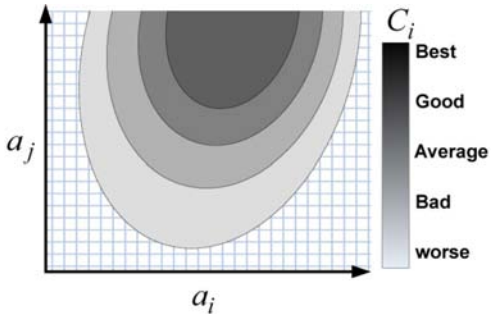

Figure 2: The optimum region touches one boundary of the graph

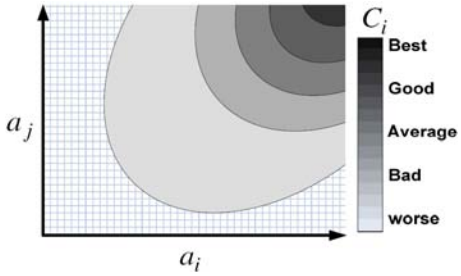

Figure 3: The optimum region touches two boundaries of the graph

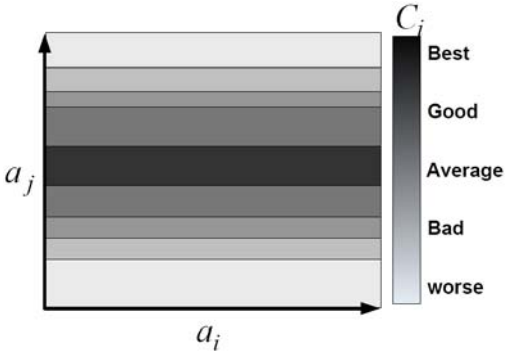

Figure 4: Changes in one of the objectives is not sensible.

2-2. Cost Function Definition

After the first round of iteration in the optimal design procedure, and finding the suitable design parameters, the next step is to determine the costs and their weights for each objective function which should be integrated to generate an overall optimization index. The main concern in the multi-objective optimization of parallel manipulators is definition from the cost functions and their weight in the optimization index [1]. VI method assists the designer to define the costs by the generated color spectrum graph as shown in figure 1. The color map of objective function C_i is divided into five regions; best (b_i1), good (b_i2), median (b_i3), bad (b_i4), and worst (b_i5). Desirable specifications can define each region boundaries. The recommended values assigned to the best and worst boundaries are possible minimum and maximum values of the objective function, respectively. The good and bad regions are minimal and maximal data found in the graphs representing the same objective function, and the *median* is calculated by the statistical median [17] of the graphs sorted data. It is recommended to use median instead of the average of the data, in case where very high or low data exist in the analyzed data, such as the rate of singular values of a robot Jacobian. In the case of using a gradient–based optimization method, polynomial curve can fit the desired quintuplet points. Therefore, such a cost function not only normalizes the output value but also determines desirable conditions for the optimization tool. The key point in this definition can be explained by the following rates of changes during the regions:

$$\left\{\forall(c_1,c_4)\left|\begin{matrix}c_1=C_i(a_i)\in(b_{i1},b_{i2})\\ c_4=C_i(a_i)\in(b_{i4},b_{i5})\end{matrix}\right.\right\}\Rightarrow\left|\frac{\partial c_1}{\partial a_i}\right|<\left|\frac{\partial c_4}{\partial a_i}\right| \quad (1)$$

$$\left\{\forall(c_2,c_3)\left|\begin{matrix}c_2=C_i(a_i)\in(b_{i2},b_{i3})\\ c_3=C_i(a_i)\in(b_{i3},b_{i4})\end{matrix}\right.\right\}\Rightarrow\left|\frac{\partial c_2}{\partial a_i}\right|<\left|\frac{\partial c_3}{\partial a_i}\right| \quad (2)$$

Such a rate order guides the solution towards feasible area while avoids forcing the other cost functions into infeasible regions. Additional to the equations 1,2, of the following two rate limitations is proposed to avoid forcing other cost functions into infeasible regions.

$$\frac{\partial c_1}{\partial a_i}<\frac{\partial c_2}{\partial a_i} \quad (3)$$

$$\frac{\partial c_4}{\partial a_i}<\frac{\partial c_3}{\partial a_i} \quad (4)$$

This idea may be implemented by fuzzy membership functions [18] or other tools, as well. Nevertheless, the simplest method is to use linear interpolation between boundary points or the equivalent polynomials as addressed in equation 26. Proposed grades and colors are assigned for each region bound as shown in table 1. Colors are used to visually inspect the graph patterns.

Table 1: Boundary values for weighting costs of objective function

Condition	Cost	Color Index	Meaning
Best(b_{i1})	0	64	Possible Ideal Value
Good(b_{i2})	10	58	Max. Graph Data
Medium(b_{i3})	30	45	Median Graph Data
Bad(b_{i4})	80	12	Min. Graph Data
Worst(b_{i5})	100	1	Possible Worse Value

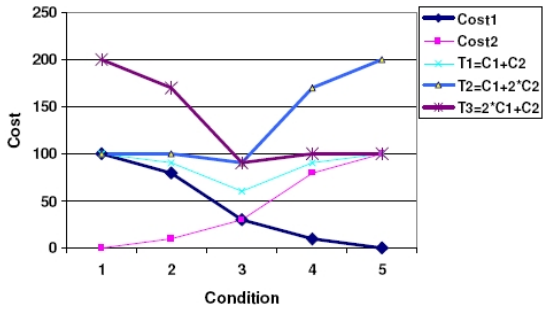

Figure 5: Optimum condition is not changed during small changes in the weights

In the worst case, assume that there exist opposite pair of objectives, as shown in figure 6 the condition 1 of the design parameters result in optimum point of cost function C'_1 while the condition becomes the worst point in cost function C'_2. Therefore, total cost function, T'_1, becomes flat. On the other hand, if the weighted summation of cost functions, such as T'_2 and T'_3 is used, the optimum point significantly changes during the weight tuning of the cost functions. we propose using a nonlinear cost function which can preserve the convexity of the problem rather than any linear weight. In the worst condition, the convexity of total cost function is more robust to opposite objectives C_1 and C_2. As shown in figure 5, even if weight of a cost function is changed, the optimum result in T_1, T_2, or T_3 doesn't meet the boundary constraints to achieve a balance in conditions. Note that, weighted summation is not used in this method and any weights in this example are used to examine the proposed cost functions robustness to nonlinearity of the objectives. The mentioned cost functions are robust to at most two conflicts in the objectives. Therefore, the other challenging problem is to find behavior of objective functions in the search boundaries. The VI method has a significant role in the determination of objectives and related cost functions and their conflicts. It warns the designer that objectives are not comparable to each other, or which design parameter is

more important for what cost function. In a practical design, usually the total cost function of the optimal design problem should become convex, since it will not be useful to have an optimum design with very large values of design parameters. Therefore, the existence of only one diverged objective function represents the ignorance of another objective or design parameter.

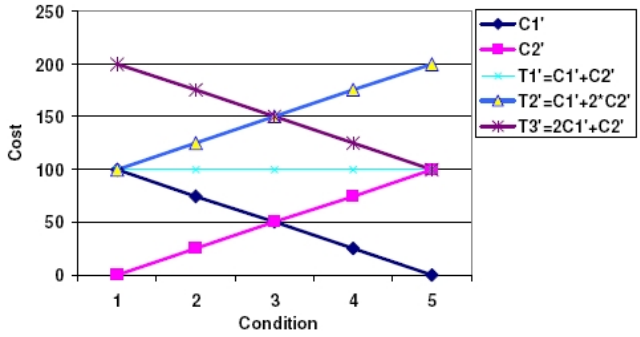

Figure 6: Optimum condition is significantly changed during small changes in the weights

Table 2 shows a typical state of relation between six cost functions and seven design parameters. In this representation *c* indicates that by minimizing the corresponding cost function an optimum value is reached for the related design parameter. Moreover, $\pm d$ denote reaching to a lower or upper limit of a parameter through minimizing the corresponding cost function. For the case shown in table 2, since no optimal solution is found for parameter a_5 for all the objectives, the constraint limit reached in optimization of cost function C_4 will be regarded as the only optimum point for this parameter. Now if the constraint is based on some physical hard limitations, it is better to set the value of this design parameter manually, and no optimization is needed to be run for this parameter. However, in many cases, the designer limits the range of the design parameters by some intuitive constraints to avoid huge or miniature dimensions in the design. In such cases, we propose replacing this limitation with a continuous cost function which describes manufacturing costs. Furthermore, as it is seen for the cost function C_5, a specific optimum is reached for the only parameter a_4. This means that this cost function is sensitive to only this parameter, and therefore, a_4 should be fixed at the optimum value for the multi objective optimization. As another typical case, the row related to parameter a_7 in this table shows that the lower limit of this parameter is reached by optimizing cost function C_1, while its upper limit is reached by optimizing cost C_6.In such case, the optimum value of this parameter can be reached by running a multi–objective cost function. This would be the case for parameter a_6, in which the number of upper limits, and lower limits reached in the results of different individual cost function optimizations are the same. Finally, optimum value for a_1 should be higher than its optimal value obtained in the optimization C_1, since one upper limit is obtained for cost function C_4, and the optimum value for a_3 would be a tradeoff between two separate optimal values obtained for cost functions C_1 and C_2.

Table 2: Dependency of the objectives on the design parameters extracted from the graphs

Objectives / Design Parameter	C_1	C_2	C_3	C_4	C_5	C_6
a_1	c	-	-	+d	-	-
a_2	-	+d	+d	-d	-	-
a_3	c	c	-	-	-	-
a_4	-	-	-	-	c	-
a_5	-	-	-	-d	-	-
a_6	+d	-d	-d	+d	-	-
a_7	-d	-	-	-	-	+d

c: converged to an optimum in the graph
+d: diverged into the positive side constraint
-d: diverged into the negative side constraint

The proposed VI method consists of plotting individual graphs and inducing the summarized table from these graphs. By this means boundaries of optimization search area can be effectively reduced to a concise feasible region, resulting in significant reduction of computation cost. This region can be chosen as wide as the median about the optimal values of the remaining parameters, due to the rate limitations enforced in equations 1 to 4. To examine the details of VI method, a real case study will be performed in next sections. Since the analyses of graphs with more than two dimensions are complicated, for brevity the graphs are always illustrated for a pair of design parameters, while the other parameters are fixed. The rate constraints on the cost functions, avoids forcing an objective function into infeasible region by another objective function, and therefore, the optimum point will remain at least in an area encapsulated by medians.

3. Optimal Design Problem for CDRPMs

3-1. General Structure Description

The general architecture of a 6 DOF, cable driven fully parallel manipulator subject to our optimal design is shown in figure 7. In this manipulator, the moving platform is supported by *m* limbs of identical kinematic structure. Each limb connects the fixed base to the manipulator moving platform by a spherical joint (S) followed by a cable represented kinematically by a prismatic joint (P) and another spherical joint (S) on the other attachment point. The kinematics structure of a prismatic joint can be used to model piston–cylinder actuator at each limb, or a more desirable cable–driven one, as in our case. As it is shown in figure 7, A_i denote the fixed attachment points of the limbs, i=1,2,…,m, B_i denote point of connection of the limbs on the moving platform, and L_i denote the limb lengths. The position and the orientation of the centroid of the moving platform G, is denoted by:

$$\mathbf{x} = \left[x, y, z, q_x, q_y, q_z \right]^T \tag{5}$$

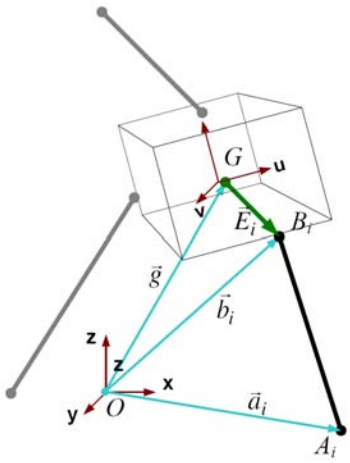

Figure 7: A general kinematic structure of CDRPMs

where, the orientation of the manipulator moving platform is denoted with respect to the moving coordinate frame. Since, the manipulator is driven by cables; at least one degree of redundancy is required to keep all the cables in tension [14]. Furthermore, in order to provide dexterous workspace for the end-effector motion, it is proposed to use at least *two* degrees of redundancy [19]. However, other properties such as catenary droop [20], flexibility [21], and vibration [22] of the cables are neglected at this stage of the optimal design. Light weight and over–constrained designs of CDRPMs avoid sagging effects using pretension in cables by means of an appropriate redundancy resolution technique [23]. However, these effects are not negligible but controllable [24], in large–scale under–constrained CDRPMs driven by heavy cables such as shown in FAST robot [20].

According to the required specifications, design parameters of an over–constrained CDRPM consist of finding the attachment positions in a three dimensional space or 3×2×*m* parameters. Assigning a set of parameter, and trying to tune them is neither feasible nor desirable, since:

- The number of design parameters is huge, resulting into very extensive computation cost that cannot be solved by the state–of–art optimization techniques.
- Manufacturing of an irregular shaped design is not desirable, since it would be complicated and expensive.
- Irregular shape of the attachment points locations affect the robot workspace. Therefore, the robot workspace becomes too complex and not representable to the end–user.

In order to reduce the complexity of the optimal design to an affordable and desirable one, the optimal design problem is simplified into a formulated structure which is obtained from the conceptual design. Additionally, in the VI method, the design parameters and their simplification are studied in detail. For the purpose of kinematics, the attachment positions are considered to be arbitrary chosen while they should be find during the design process.

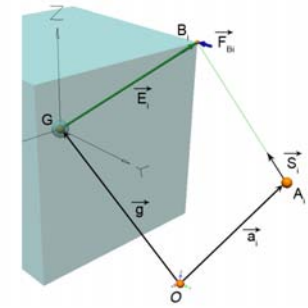

Figure 8: *i*th Attachment point on the moving platform and related vectors

3-2. Inverse Kinematics

Similar to other parallel manipulator, CDRPM has a complicated forward kinematic solution. However, the inverse kinematic analysis is sufficient for dynamic modeling. As illustrated in figure 12, the B_i points lie at the vertexes of the cube. For inverse kinematic analysis of the cable driven parallel manipulator, it is assumed that the position and orientation of the moving platform

$x=[x_G, y_G, z_G]^T$, ${}^AR_B$ are given and the problem is to find the joint variable of the CDRPM, $\mathbf{L}=[L_1, L_2, \ldots, L_m]^T$. From the geometry of the manipulator as illustrated in figure 8 the following vector loops can be derived:

$$ {}^A\overrightarrow{A_iB_i} + {}^A\mathbf{a}_i = {}^A\mathbf{g} + \mathbf{E}_i \tag{6}$$

in which, the vectors $\mathbf{g}, \mathbf{E}_i$, and $\mathbf{a}_i$ are illustrated in figure 8. The length of the *i*'th limb is obtained through taking the dot product of the vector $\overrightarrow{A_iB_i}$ with itself. Therefore, for *i*=1, 2,…, *m*:

$$L_i = \left\{[\mathbf{g}+\mathbf{E}_i-\mathbf{a}_i]^T[\mathbf{g}+\mathbf{E}_i-\mathbf{a}_i]\right\}^{\frac{1}{2}}. \tag{7}$$

3-3- Jacobian

Jacobian analysis plays a vital role in the study of robotic manipulators. Let the actuated joint variable be denoted by a vector $\dot{\mathbf{L}}$ and the location of the moving platform be described by a vector $\dot{\mathbf{x}}$. Then the kinematic constrains imposed by the limbs can be written in the general form $f(\boldsymbol{x}, \boldsymbol{L})=\mathbf{0}$ by differentiating with respect to time, we obtain a relationship between the input joint rates and the end-effector output velocity as follows:

$$J_x\dot{\mathbf{x}} = J_L\dot{\mathbf{L}} \tag{8}$$

where $J_{\mathbf{x}} = \frac{\partial \mathbf{f}}{\partial \mathbf{x}}, J_{\mathbf{L}} = -\frac{\partial \mathbf{f}}{\partial \mathbf{L}}$. The derivation above leads to two separate Jacobian matrices Hence the overall Jacobian matrix *J* can be written as:

$$\dot{\mathbf{L}} = J\dot{\mathbf{x}} \tag{9}$$

where $J = J_L^{-1}J_{\mathbf{x}}$. Jacobian matrix not only reveals the relation between the joint velocities $\dot{\mathbf{L}}$ and the moving platform velocities $\dot{\mathbf{x}}$, but also constructs the transformation needed to find the actuator forces t from the forces acting on the moving platform $\mathbf{F}$. When J_L is singular and the null space of J_L is not empty, there exist some nonzero $\dot{\mathbf{L}}$ vectors that result zero $\dot{\mathbf{x}}$ vectors which called serial type singularity and when J_x becomes singular, there will be a non-zero twist rate $\dot{\mathbf{x}}$ for which the active joint velocities are zero. This singularity is called parallel type singularity [1]. In this section we investigate the Jacobian of the CDRPM platform shown in figure 12. For this manipulator, the input vector is given by $\mathbf{L}=[L_1, L_2, \ldots, L_m]^T$, and the output vector can be described by the velocity of the centroid *G* and the angular velocity of the moving platform as follows:

$$\dot{\mathbf{x}} = \begin{bmatrix} \mathbf{V}_G \\ \boldsymbol{\omega}_G \end{bmatrix} \tag{10}$$

Jacobian matrix of a parallel manipulator is defined as the transformation matrix that converts the moving platform velocities to the joint variable velocities, as given in equation 9. Therefore, the CDRPM Jacobian matrix J is a non-square *m*×*n* matrix. The Jacobian matrix can be derived by formulating a velocity loop-closure equation for each limb. Referring to figure 8, a loop-closure equation for the *i*th limb is written in equation 6. In order to obtain the Jacobian matrix, let us differentiate the vector loop equation 6 with respect to time, considering the vector definitions S_i and $\mathbf{E_i}$ illustrated in figure 8. Hence, for *i*=1,2,$\mathbf{L}$,*m*:

$$\mathbf{V_G} + \boldsymbol{\omega}_G \times \mathbf{E_i} = \dot{L}_i\hat{S}_i + L_i(\boldsymbol{\omega}_i \times \hat{S}_i) \tag{11}$$

Furthermore $\boldsymbol{\omega_i}$ denotes the angular velocity of *i*'th limb with respect to the fixed frame *A*. To eliminate $\boldsymbol{\omega_i}$, dot-multiply both sides of equation 11 by $\hat{S}_i$.

$$\dot{L}_i = \hat{S}_i\mathbf{V}_G + (\mathbf{E}_i \times \hat{S}_i)\boldsymbol{\omega}_G \tag{12}$$

Rewriting equation 12, in a matrix form:

$$\dot{L}_i = \begin{bmatrix} \hat{S}_i & \mathbf{E}_i \times \hat{S}_i \end{bmatrix} \cdot \begin{bmatrix} \mathbf{V}_G \\ \boldsymbol{\omega}_G \end{bmatrix} \tag{13}$$

Using equation 13 for *i*=1,2,…,*m*, the CDRPM Jacobian matrix J is derived as following.

$$J\dot{\mathbf{x}} = \begin{bmatrix} \hat{S}_1^T & (\hat{E}_1 \times \hat{S}_1)^T \\ \hat{S}_2^T & (\hat{E}_2 \times \hat{S}_2)^T \\ \vdots & \vdots \\ \hat{S}_m^T & (\hat{E}_m \times \hat{S}_m)^T \end{bmatrix} \cdot \begin{bmatrix} \mathbf{V}_G \\ \boldsymbol{\omega}_G \end{bmatrix} \tag{14}$$

Note that the CDRPM Jacobian matrix J is a non-square *m*×*n* matrix, since the manipulator is a redundant manipulator. If the manipulator has no redundancy in actuation, the Jacobian matrix, J was squared and the actuator forces can be uniquely determined by $t = J^{-T}\mathbf{F}$, provided that J is nonsingular. For redundant manipulators, however, there are infinity many solutions for τ to be projected into $\mathbf{F}$. The simplest solution would be a minimum norm solution, which is found from the pseudo–inverse of J^T, by $t_0 = J^{T^\dagger}\mathbf{F}$. This solution is implemented in the simulation studies reported in this paper. Other optimization techniques can be used to find the

actuator forces projected from $\mathbf{F}$ which can minimize a user defined cost function [25] by applying a set of actuator forces with zero resultant torque:

$$t = t_0 + \left(I_{m\times m} - J^{T^\dagger} . J^T \right) \boldsymbol{\gamma} \tag{15}$$

In conclusion, the affecting forces of the end–effector have two sources, the Jacobian matrix projection and null space of the Jacobian. Therefore, in the design process of a CDRPM, both sources should be analyzed. In the third section, dexterity measures are introduced as indices for the analysis of the first term, while tension force feasibility focuses on the analysis of the second term of equation 15.

4. Optimal Design Objectives

4-1. Dexterity

In the robotic community literature many dexterity measures have been introduced to assist the design of serial and parallel robots and to correlate different behaviors. Some problems exist to define a global dexterity measure for a manipulator. If the dexterity measure is changed by pure scaling of the robot dimensions, final result of an optimal design leads to a miniature– or huge–scale manipulator and even dimension may affect the optimal condition. Therefore, a scale independent measure is needed which is studied in various comprehensive researches. Some well–defined dexterity measures have been introduced for serial and parallel manipulators [26]. Moreover, Merlet reviewed most of the manipulability and dexterity measures for parallel manipulators in [27]. His latest comprehensive review leads to focus on dexterity indices as an open problem. Additionally, in his opinion, the most appropriate global accuracy indices are the determination of the maximal positioning errors, their average values, and their variance.

On the other hand, dependence of the moving platform angular velocity $\boldsymbol{\omega}_\mathbf{G}$ coefficient, on the dimensions of the arm vectors, $\mathbf{E}_i$ s as depicted in equation 14, leads to scale dependency of the parallel manipulator Jacobian matrix. This scale dependency significantly affects all the conventional dexterity indices. Thus, some of optimal design researches eliminate scale dependency of the Jacobian matrix, before implementing any analysis on the dexterity measure. For serial spatial manipulators, Gosselin [26] proposes to assume three virtual points as vertices of a triangle on the end-effector and to build a Jacobian matrix for their translational velocities. Furthermore, the method is extended for a conventional parallel mechanism like Stewart-Gough platform by Kim and Ryu [28]. Although the method is useful for the Stewart-Gough platform, it is not generally applicable in cases where the attachment points are located spatially in space, In other words, for a manipulator with spatial shaped end-effector, at least four virtual points are required to modify the Gosselin's method and determine effects of attachment point replacement, while it is almost impossible to avoid rank deficiency during the mapping. Therefore, before starting the dexterity measure analysis, in this section a normalized Jacobian is defined, which is generated by substitution of all $\mathbf{E}_i$ s with their normalized form $\hat{\mathbf{E}}_i$ s. This change immediately results into a scale independent Jacobian matrix for a fully parallel spatial manipulator like the KNTU CDRPM:

$$J = \begin{bmatrix} \hat{S}_1^T & (\hat{E}_1 \times \hat{S}_1)^T \\ \hat{S}_2^T & (\hat{E}_2 \times \hat{S}_2)^T \\ \mathbb{M} & \mathbb{M} \\ \hat{S}_m^T & (\hat{E}_m \times \hat{S}_m)^T \end{bmatrix} \tag{16}$$

in which,

$$\hat{E} = \frac{1}{\left\| \mathbf{r} \right\|} \mathbf{r} E \tag{17}$$

However, this is conditionally applicable, and only if the manipulator uses a fixed size of $\mathbf{E}_i$ vectors, the normalized Jacobian is useful for optimization. Hence, the occupied volume of the end–effector should be either considered fixed or used as an individual cost function. By this means, any dexterity index can be used as an appropriate cost function, in which a variety of dexterity indices are proposed in the literature. In this paper we have used the condition number [5] as one of the proposed dexterity measures in our design. This choice is desirable, since it is scale independent. Moreover, the range of condition number from [1…∞] is mapped into [0…∞] by the following transformation:

$$CN = \frac{s_{\max}}{s_{\min}} - 1 \tag{18}$$

in which, σ_{max} is the largest and σ_{min} is the smallest singular value of the appropriate Jacobian matrix. Therefore, in an optimal design it is suitable to have *Cn*=0, which describes an isotropic design in a given position. Moreover, a large value for the condition number indicates being close to singular configuration. By calculation of this index at each grid point of the workspace, the dexterity condition of all configurations of the workspace can be determined. Furthermore, in the optimal design processes it is necessary to analyze dexterity condition of the manipulator throughout

the entire workspace. Therefore, a global condition index is required to examine both the dexterity and the homogeneity of all points of the workspace simultaneously. There are two global indices introduced for manipulator dexterity.

$$GCI = \frac{\int_w CN dW}{\int_w dW} \tag{19}$$

GCI is the integral based global condition index where *CN* is the condition number and *W* is the workspace [29]. The *GCI* validity is questionable when the workspace contains singular points. This drawback is solved by Monte Carlo integration [30]. However, this index is not able to provide any lower or upper bounds on the dexterity in the workspace. For this means another definition for global condition number is introduced as following:9

$$GC = \frac{\max(s_{\max_i})}{\min(s_{\min_i})} \tag{20}$$

In which, $\max(s_{\max_i})$ and $\min(s_{\min_i})$ are the global maximum and minimum singular values of the Jacobian matrix through the entire workspace, respectively. If the *Global Condition Number* (GC) approaches to 1, the workspace is more dexterous and homogeneous, and for large values for GC, the manipulator is less dexterous. Note that both *GC* and *GCI* indices are tractable in a singular free workspace. In general they cannot show the extent of the singular configurations within manipulator workspace. Therefore, another cost function is needed to be defined to quantify the extent of the singular points. In the CDRPMs, such a cost function can be combined with the evaluation of force feasible workspace, which is defined in next subsections.

4-2. Collision Free Workspace

Enlargement of the dexterous workspace results into an over constrained design of CDRPMs [19]. Thus, the cables are distributed throughout the entire manipulator workspace, and it may cause various collisions. On the other hand, the cables locations vary according to the end-effector position. Therefore, collision detection of the CDRPM is not similar to that of serial manipulators. Collision detection and obstacle avoidance techniques are addressed in several researches on serial manipulators and mobile robots. However, few studies had been done on the CDRPM structures [31]. Moreover, CDRPMs have large orientation workspace compared to that of the conventional parallel manipulators, and therefore, collision detection is more important in the process of determining the workspace of CDRPM [32]. The cables may collide with each other, or with the end-effector body. Therefore, two collision detection algorithms are used which are fully described in [32, 33] to determine accessibility of a point inside the basic workspace in a collision free status. After running these algorithms for a grid point of manipulator workspace, the accessible percentage of the workspace as proposed by [30] can be calculated by the following equation:

$$VP = \frac{\text{AccessiblePoints}}{\text{Bounding Box Volume}} \tag{21}$$

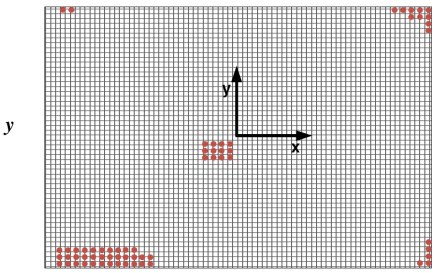

Figure 9: There exist some inaccessible points near the workspace center

The next issue in the analysis is to examine *total orientation workspace* (TOW) [34]for a six DOF manipulator. If a six DOF grid is used to obtain the TOW, the number of the grid points becomes of sixth order of the resolution, and therefore, enormous for any numerical process. Accordingly, it is necessary to use a set of *constant orientation workspace* (COW) analysis. The constant orientation workspace (COW) is defined as the three dimensional region that can be attained by the moving platform's centroid when it is kept at a constant orientation [35]. Due to process costs, the TOW examination should be replaced with a set of fixed orientations which are extracted from required boundaries for orientation.

Furthermore, the locations of inaccessible poses can affect the performance of the manipulator. Although in an appropriate collision free workspace, few collisions may occur, collection of inaccessible points at the middle of the task space is more annoying for a variety of tasks as shown in figure 9. By intuitive comparison of two figures 9 and 10, the latter shows a better situation, while proposed indices introduced in [32] or [31] gives a better condition for figure 9. This is solely due to the fact that the number of the inaccessible points is considered in them and not the location of them.

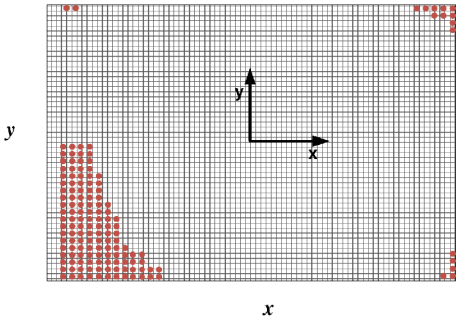

Figure 10: All of the inaccessible points are located near boundaries

Thus, it is better to define a cost function to incorporate both the number and the location of the inaccessible points. By examination of various distance costs, the proposed objective function is proposed using *rms*:

$$\mathrm{rms}(x_i) = \sqrt{\frac{1}{g}\sum_{i=1}^{n} x_i^2} \qquad (22)$$

in which, g is the number of inaccessible grid points, and x_i is the distance to the central configuration. For each axis of the workspace, normalized RMS of the inaccessible points should be by the so called *distance cost* (DC) as following:

$$\mathrm{DC} = \frac{x_{\max}}{rms_x} + \frac{y_{\max}}{rms_y} + \frac{z_{\max}}{rms_z} \qquad (23)$$

where, $x_{\max}$, $y_{\max}$,$z_{\max}$, are dimensions of the smallest workspace bounding box in each coordinate axis. Moreover, another analysis on the Jacobian matrix is necessary for the CDRPMs.

4-3. Force Feasible Dexterous Workspace

In the subsection **Error! Reference source not found.** dexterity measures are discussed, which are usually the only main index for usual conventional manipulators. Note that, dexterity is *"the ability to arbitrarily change the end-effector position and orientation, or apply forces and torques in* any arbitrary *directions in the workspace"* [36]. However, in the cable driven manipulators dexterity measures should include an inequality constraint on the cable forces to guarantee tension forces in the cables while maneuvering. This analysis is called force feasibility analysis, in which we try to detect whether dexterity is available using tension forces or not. Moreover, the volume of the tension force feasible dexterous workspace, which we call it FFDW becomes an objective for the optimization problem. Hence, a method is required to judge about force feasibility and then about its volume and location within the workspace. Various comprehensive methods were proposed to calculate tension force feasibility for a spatial CDRPM. [37, 38, 39] introduce analytical, geometrical, and numerical solutions in order to determine reachable force feasible workspace from the Jacobian matrix. Nevertheless, in these researches only one *degree of redundancy* (DOR) is used while in a seven actuated CDRPM, or six actuated in addition to a passive force [12], dexterous workspace cannot be analyzed, and just reachable workspace [40] could be analyzed. On the other hand, few studies are developed to include more than one degree of redundancy (DOR). A method was proposed by Williams and Gallina [41] for at most two DOR in CDRPM structure. Moreover, FFDW of CDRPMs was extracted by a method proposed by Gosselin et.al [16]. However, both recent researches were suggested only for planar CDRPMs and analysis of the FFDW for spatial CDRPMs is still an open problem [16]. Therefore, a FFDW determination method is necessary to propose for over–constrained spatial CDRPMs. To examine force feasibility of the robot, projection feasibility by the Jacobian matrix, J against an external force vector acting on the moving platform wrench, $\mathbf{W}$, on the cable's tension force directions, $\mathbf{F}$, should be studied. Note that:

$$-J^T\mathbf{F} = \mathbf{W} \qquad (24)$$

The result of the analysis strongly depends on the *n*–dimensional force and torque vector which will be projected by the Jacobian which is neglected in the most of researches like [42]. In some researches, wrench of gravity effects is used [43] which verifies whether the robot can rest at a pose or not. The problem is highlighted in a method proposed by Barrette and Gosselin [44] that advises to include dynamical properties of the CDRPM instead of gravity. Nevertheless, while these methods use a constant vector in the Cartesian space, they cannot fulfill requirements of dexterity verification. Hence, they are only useful to discover statically reachable force feasible workspace or feasibility of motion along a fixed direction. In other words, there is a great deal of variation among the role of each cable in motion along the same axis depending on the end–effector position. Thus, a fixed vector in the Cartesian space cannot be an appropriate wrench for examination of force feasibility. The favorable analysis is to warranty making any arbitrary resultant wrench by the cables tension forces within the determined dexterous workspace.

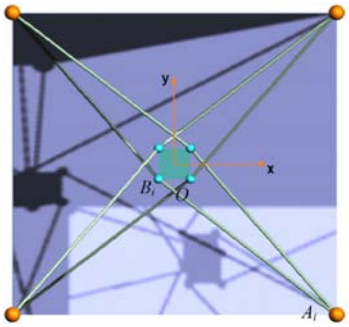

Figure 11: The KNTU CDRPM, a top view

Notice that the elements of the Jacobian matrix in 14 enlighten an important insight about the projection of forces on the moving platform. The *i*'th row of the Jacobian matrix corresponds to a wrench exerted on the center of mass and along the direction of the *i*'th cable, $\hat{S}_i$ whose resulting torque that can be determined by $\mathbf{E}_i \times \hat{S}_i$. Therefore, the worst condition for the force feasible workspace of a CDRPM is when such wrench is exerted on the end-effector, i.e. exactly in the direction of one of the cables at the center of mass. Such extreme wrenches can be easily calculated by the *i*'th row of the Jacobian matrix:

$$\mathbf{W}_i = \begin{bmatrix} \hat{S}_i \\ \mathbf{E}_i \times \hat{S}_i \end{bmatrix} \tag{25}$$

Repeating projection of $\mathbf{W}_i$ for each cable direction by the redundancy resolution methods [45] or any method for feasibility of the projection [19, 38], *i*=1,2,…,*m* determines whether a full-ranked Jacobian in a pose is force feasible or not. Feasibility of exerting a force or torque by serial or rigid-linked parallel manipulators is studied in dexterity analysis. According to the definition, traditional dexterity measures are not sufficient for CDRPMs. Therefore, force projection feasibility of the proposed wrench, $\mathbf{W}$ should be the most important factor in the dexterity analysis of the CDRPMs instead of the typical dexterity measures. If exerting a force in the direction of vs becomes impossible, there exists at least one inaccessible direction of motion. Such condition contradicts the dexterity of the robot, although the contemporary measures of dexterity or manipulability show a good condition for the Jacobian matrix. Therefore, having a good condition number alone is not sufficient to ensure the dexterity of a CDRPM. We propose to define dexterous workspace for a redundant cable-driven manipulator as the FFDW when the worst case wrench is exerted on the manipulator. If such wrench is applied to the robot in the direction of a cable, that cable is not capable to produce any positive reaction to the end-effector. Therefore, one degrees of redundancy of the robot is simply annihilated, and in order to achieve dexterous workspace, *at least* two *degrees of redundancy* is required. Thus, the main application of this objective is where the robot has more than one DOR.

Next, the worst case wrench projection feasibility should be analyzed over the entire workspace to determine inaccessible points by special projection methods. This examination can be done together with collision free workspace procedure. Therefore, 21 is revised such that the accessible points are out of tension force infeasible points. However, the quantized condition of robot changed into a Boolean logic condition. Thus, analysis of traditional condition number cannot be ignored. Otherwise, amounts of the cables tension forces should be studied. Furthermore, this function may increase effect of the condition number especially when some singular points exist within the workspace.

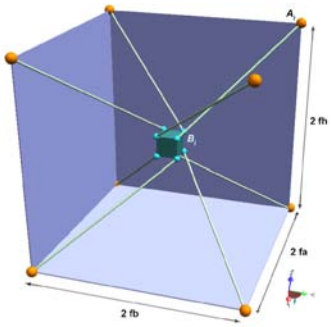

Figure 12: The KNTU CDRPM, a perspective view

5. Case Study: KNTU CDRPM

Design of the KNTU CDRPM is a multi objective optimal design problem such as other CDRPMs which has two DOR. This six DOF manipulator is under investigation for possible high speed and large dexterous workspace applications such as laser welding. Its design is suitable for long–time high acceleration motions. In this section, application of the VI method and the cost functions is studied in detail. Firstly, a formulated design problem is defined. Then, the VI method is applied to achieve objective functions and design parameters. The resultant graphs are analyzed to determine suitable parameters. Finally, a numerical optimization method is used to find the optimum parameters for the given cost functions.

5-1. Problem Statement

In the optimal design process of the KNTU CDRPM, two main subjects should be studied in detail: objective criteria and design parameters. In other words, designer answers these questions: Which properties are needed for the task of the manipulator? Which parameters can be changed inside their interval to achieve such properties? There are various types of optimality measures for CDRPMs as mentioned above. All of the measures described in the third section are used during the VI process of the KNTU CDRPM. However, percentage of the accessible workspace in a regular-shaped, condition number, and its occupied volume have more significant impression in the choosing design parameters as shown by VI graphs. Therefore, the process of numerical optimization involves these three objectives. For Both of the dexterity and workspace measures exploration of a six dimensional grid is required. Numerical search of this grid is computationally expensive especially for the calculation of collision free and tension force feasible workspace. On the other hand, as shown in [32], accessible workspace with 30^{O} rotation of the end–effector is located inside the accessible workspace while the end–effector has 15^{O} rotation around the same axis. Therefore, variety of rotations assumed for the extraction of the COWs and their intersection subspace. Roll, pitch, and yaw angles are changed for each translational space grid as: (0,0,0), (30,0,0), (30,30,0), (–30,30,0), (0,30,0), (0,0,10), (0,0,–10). This test is repeated for all of the grid points with 7^{cm} resolution.

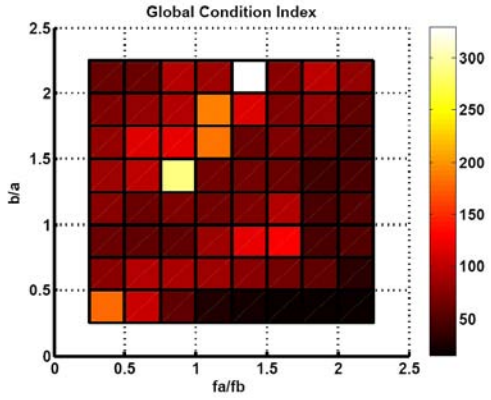

Figure 13: Variation of the GCI versus a pair of design parameters: hot color map

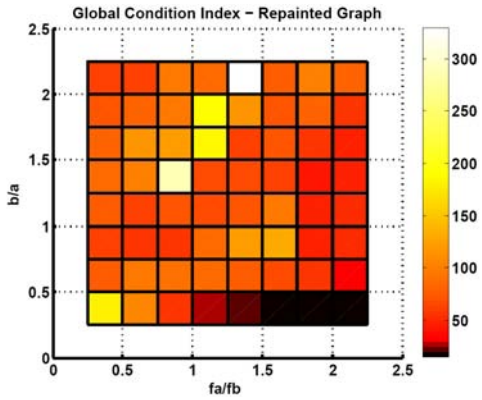

Figure 14: Variation of the GCI versus a pair of design parameters: rearranged hot color map

The optimal design problem of the KNTU CDRPM is reduced to search for dimensions of two rectangular parallelepiped frames. The fixed attachment points, A_i, are located on the vertexes of the fixed frame while the moving attachment points are placed positioned right at the vertexes of the moving frame as shown in figure 12 as well as B_i points on the moving rectangular parallelepiped frame. This reduction is necessary to reach the benefits mentioned in subsection **Error! Reference source not found.**. Therefore, six design parameters are defined as below:

1. *fa*: half of length of the fixed frame or dimension of the box along *x* axis with respect to the fixed coordinate.
2. *fb*: half of width of the fixed frame or dimension of the box along *y* axis with respect to the fixed coordinate.
3. *fh*: half of the height the fixed frame or dimension of the box along *z* axis with respect to the fixed coordinate.
4. *a*: half of length of the moving frame or dimension of the box along *x* axis with respect to the moving coordinate.
5. *b*: half of width of the moving frame or dimension of the box along *y* axis with respect to the moving coordinate.
6. *h*: half of the height the moving frame or dimension of the box along *z* axis with respect to the moving coordinate

According to figure 11, position of the attachment points are symmetric along *x* and *y* at top view of the manipulator in the conceptual design. Therefore, parameters ratio, *fa*/*fb* and *a*/*b* is used during the optimization. This simplification not only reduces design parameters and complexity of

optimization, but also decreases the effects of the not normalized $\mathbf{E}_i$ vectors in the rotation side of the Jacobian, equation 14. To set specific amounts for each parameter, volume of the end–effector is set to a constant value ($8h/100$) as well as the fixed attachments' frame volume ($8\times2\times fh$).

5-2. Visual Inspection Graphs and Costs

According to the mentioned design parameters and objectives, a VI graph is illustrated as shown in figure 13 using a normally distributed hot color map. Note that, each point of the graph is the result of an exploration of entire workspace of the manipulator. Next, the color map is modified as addressed in table 1 to illustrate the graph as shown in figure 14.

This modification lead to show the good region more clearly while color gradient in the bad and the median regions are decreased. In this step, validation of optimum region, dependency, and convexity of the functions are checked by an visually inspection by designer. For instance, change of the GCI versus dimensions of the fixed frame along *x* and *y* axes, *fa* and *fb*, can be shown in figure 15 while $\frac{a}{b}=1$.

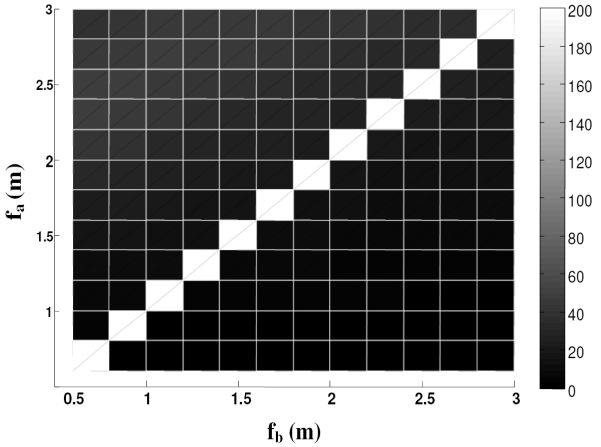

Figure 15: Variation of the GCI versus *fa* and *fb*:hot color map

This figure clearly shows an ill condition in which *fa* is equal to *fb*. Further studies show that this problem becomes serious especially when *a.fa=b.fb*. To clarify this problem, let's view the result of scanning on the *x*=0 plate in figure 16.

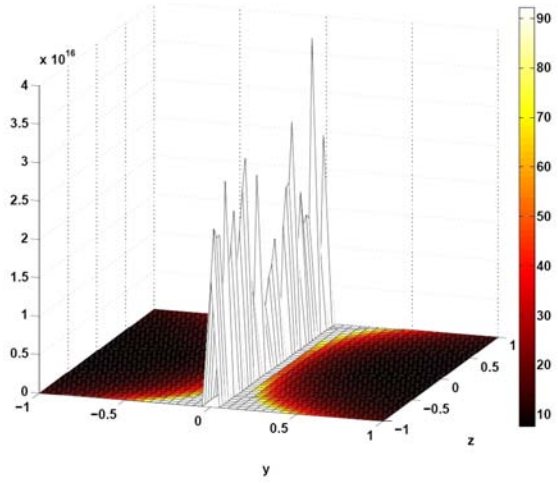

Figure 16: Condition number on *x*=0 plane

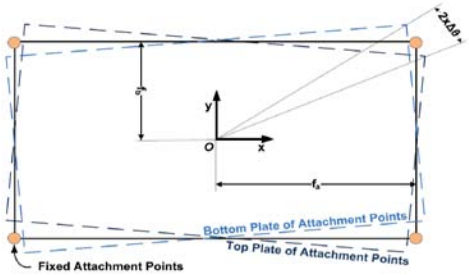

Figure 17: Changed design parameters

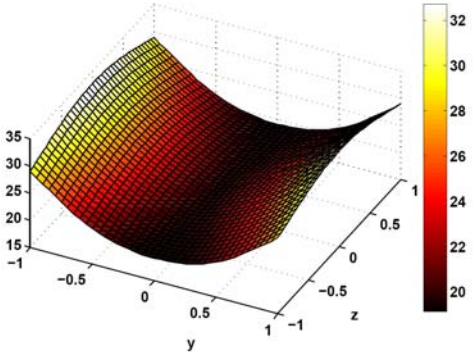

Figure 18: The condition number values on the *x*=0 after the change in design parameters

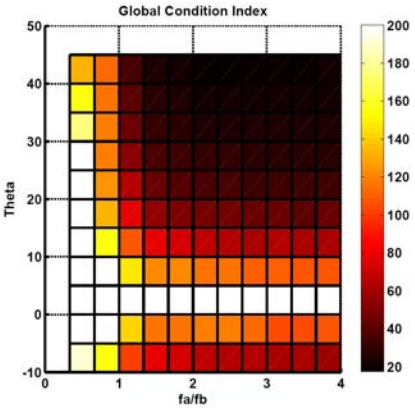

Figure 19: Dependency of global condition number on the design parameters

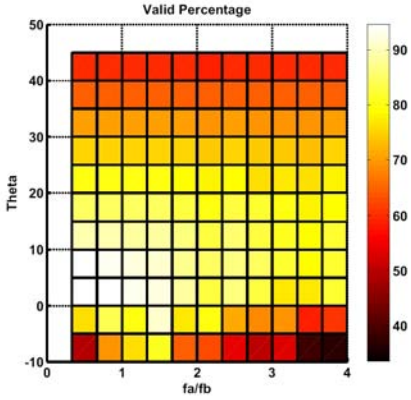

Figure 20: Dependency of collision free workspace on the design parameters

As can be seen, singularity exists within the workspace of the robot. Analysis of the Jacobian condition in the singular positions shows that a major problem exists in the Neuron design of the KNTU CDRPM; rotation about *z* axis of the end-effectors which strongly depends on the translation along *z* axis especially in the central locations of the workspace. In other words, linear independency of 4*th* and 6*th* columns of the Jacobian fails in the *z*=0 plane and the Jacobian rank deficiency disturbs motion control of the robot at this position. Therefore, rearrangement of the attachment points is necessary to decouple the role of the cables in translations and rotations of the end-effector. Since the shape of the end-effector is suitable to avoid cable to body collision [32], arrangement of the fixed attachment points should be studied.

To achieve a better condition number on the *z*=0 plane, we had to disturb symmetric arrangement of the fixed attachment points, A_is. This change is applied to the width to length ratio of the fixed frame and rotation of the top and bottom plates about *z* axis as shown in figure 17. By this means the symmetricity and role dependence of the cables can be remedied by changing *fa*,*fb*,θ. Effects of changing these parameters on the GCI are illustrated in VI graph 19. Analysis of the results shows that:

- Increment of θ has significant role in the singularity avoidance within the workspace.
- Equal *fa* and *fb* values, and near zero values of θ lead to singularity of the manipulator.
- There exists a region in the results where the manipulator workspace is singular free.

However, the values of design parameters θ, f_a and f_b cannot set to the ideal values because another limitation may significantly decrease the workspace of the robot. Cable to cable and cable to end-effector collisions can bound the end-effector motion. Extracting another VI graph 20 shows that *the best global condition number region located in the worst collision free workspace* and vice versa. Therefore, this phenomenon denotes that θ should be added to the design parameters.

Furthermore, this opposite condition for each value of the design parameters emphasizes the mentioned weighting problem for multi objective optimal design problem. Therefore, weighting function is utilized as noted in subsection **Error! Reference source not found.** using the values given in table 3. A linear interpolation between boundaries is used as a simplest way to implement the rules described in equations 1 and 2:

$$y=\begin{cases}\dfrac{(x-x_w)(y_b-y_w)}{(x_b-x_w)}+y_w, & x_w<x<x_b\\ \dfrac{(x-x_b)(y_m-y_b)}{(x_m-x_b)}+y_b, & x_b<x<x_m\\ \dfrac{(x-x_m)(y_g-y_m)}{(x_g-x_m)}+y_m, & x_m<x<x_g\\ \dfrac{(x-x_g)(y_B-y_g)}{(x_B-x_g)}+y_g, & x_g<x<x_B\end{cases} \quad (26)$$

in which *x* is input value for cost function, *y* is the calculated cost. Moreover, x_w, x_b, x_m, x_g ,and x_B denote input values for the variables in worst, bad, medium, good, and best conditions for each objective function given in the table 3. y_w, y_b, y_m, y_g ,and y_B are the proposed costs from the first column of table 3 which stands for costs of worst, bad, medium, good, and best conditions, respectively.

Table 3: Boundary values for weighting costs of objective functions in figures 21, 22, 23,and 24

	Cost(y)	Condition Number	Valid%	Volume (m^3)
Worse(x_w)	100	1000	0	5
Bad(x_b)	80	329.4533	1.3636	1.3681
Mid(x_m)	30	70.2489	6.4815	0.5985
Good(x_g)	10	15.4932	15.5556	0.342
Best(x_b)	0	5	100	0

After this calculation, the resultant graph for the figure 13 will be the graph illustrated in figure 25. On the other hand, as can been seen in figure 19 dexterity criteria forces the optimum point to reach dimension constraints for θ corresponding to the pattern explained in figure 3. In order to prevent such undesirable situation, occupied volume cost is used:

$$\text{Volume} = fh \cdot \max\left(fa\sin q, fb\sin q\right) \cdot \max\left(fa\cos q, fb\cos q\right) \quad (27)$$

Consequently, weighted cost functions are shown in figures 21, 22, and 23 and the total cost function calculated by their total average, can be seen in figure 24. Analysis of these graphs clarifies the benefits of using the proposed weighting functions:

- Diverged graph of the GCI is fixed by another desirable objective function, occupied volume, to prevent touching dimension constraints which results a huge or tiny manipulator.
- Undesirable singular condition of the robot for a set of design parameters, a/b and fa/fb is found and analyzed. It is solved by addition another design parameter, θ.
- Total cost function is not diverged even if two diverged cost functions, such as GCI and Volume, exist in the optimal design criteria. convex
- Weighted cost function not only guides the optimization result in a desirable manner but also gives insight into dependency of objectives on the parameters in a VI graph.
- Total cost function introduces a trade–off between objectives.

As an example for the last item, $(fa/fb, q) = (2, 36^\circ)$ is the minimum point of GCI cost in figure 21, $(fa/fb, q) = (2, 15^\circ)$ is that of VP in figure 22, and $(1.2, 0^\circ)$ is the minimum of the graph in figure 23. However, the optimum point showed in total cost function, figure 24, is not the same point as previous graphs and it is located in $(2.2, 21^\circ)$ this set of design parameters are not the best of each graph. However, it has acceptable values in all of them as a result of the proposed weighting functions. Furthermore, summarizing the information of the graphs in table 4 shows effects of the objective functions and design parameters on each other. This table can be analyzed with the description of table 2. As it can be seen, all of the design parameters have at least one converged region and they fit in the subsection **Error! Reference source not found.** rules except *h*. Therefore, volume of the end–effector is fixed to prevent divergence of this parameter.

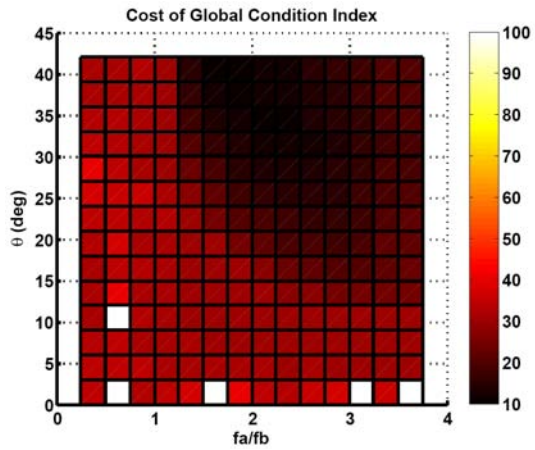

Figure 21: Weighted cost for the global condition index versus a pair of design parameters.

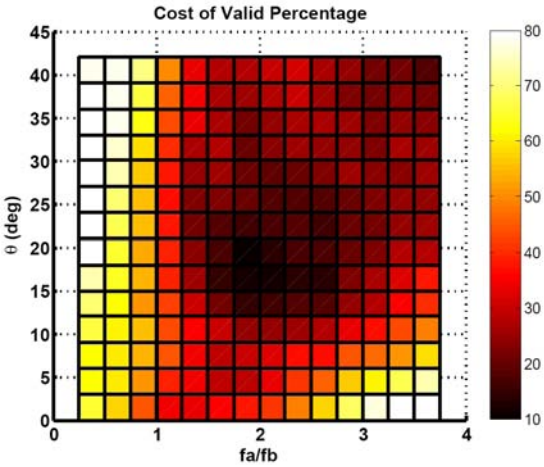

Figure 22: Weighted cost for the accessible workspace wideness versus a pair of design parameters.

5-3. Optimization

Finally, after verification of design parameters and criteria, an optimization method is required to find optimum values for the overall cost function. Because the multi objective problem is condensed into a single objective optimality problem, various optimization methods are able to find the desired parameters. The most idealistic methods are analytical methods. Since latest determination methods for feasible workspace are semi-analytical [38] and they are numerical for collision free workspace [32], for a CDRPM it is not possible to solve this problem analytically. Moreover, for this case study, gradient–based methods are not suitable, mainly because the search space is quantized by grids and fitness function is not well behaved. Therefore, grid–based and intelligent search methods are suitable for this problem such as *Genetic Algorithm* (GA) or *Pattern Search* (PS) methods or their combination [46, 47].

Practically, because of the existence of local minima, GA method is more suitable to solve this problem. However, its random behavior results into different answers during various executions for the same fitness function. This problem can be fixed by running a PS algorithm started from the GA solution. This process results to a unique answer for the design problem. This procedure is applied for our problem in hand, and the final design parameters are obtained as $\frac{fa}{fb}=1.6, \frac{a}{b}=2.2,\ fh=0.85m, h=0.17m$, and $\theta=18^{o}$ which has ±3% tolerance. Furthermore, the result of this examination shows that the manipulator workspace is about 68% without rotation of the end-effector and 55% when the end-effector rotates 20^{o} about its *x* or *y* axis. This workspace is singular free and much larger compared to that of a similar eight actuator CDRPM [9].

Table 4: Dependency of the objectives on the design parameters for KNTU CDRPM

Design Parameter	Condition Number	Valid Percentage	Volume
$\frac{a}{b}$	+d	c	-
h	+d	+d	-
$\frac{fa}{fb}$	c	+d	c
fh	-d	c	-d
θ	+d	c	-d

c: converged to an optimum in the graph
+d: diverged into the positive side constraint
-d: diverged into the negative side constraint

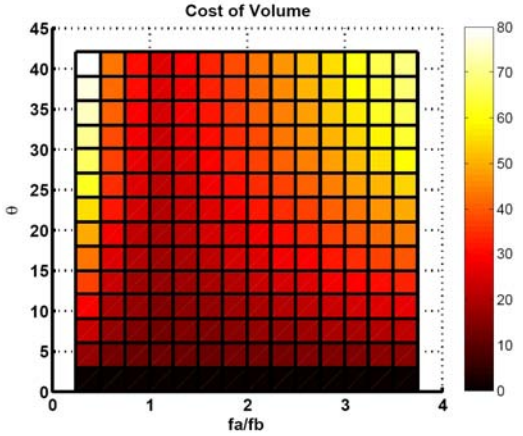

Figure 23: Weighted cost for the occupied volume versus a pair of design parameters.

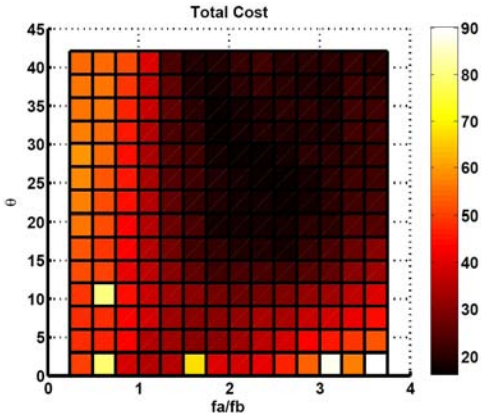

Figure 24: Weighted total cost versus a pair of design parameters.

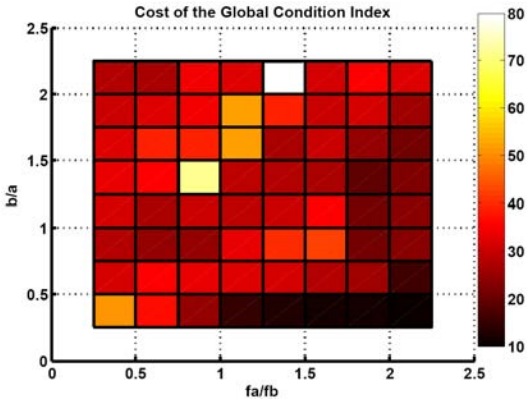

Figure 25: Weighted cost for the global condition index versus the frames dimensions ratios.

6. Conclusions

In this paper, optimal design of cable driven redundant parallel manipulators (CDRPMs) is studied in detail. This problem is formulated as a multi objective optimization for a set of design parameters and criteria. For this purpose, a brief review of various design criteria for CDRPM is discussed. *Visual Inspection* method is proposed which includes steps to illustrate potential dependency of parameters and provides insights into the optimal design process. Then, an approach for weighting of cost functions is proposed which is the most important step in the optimal design.

To illustrate utilization of these methods and to extensively discuss on the objectives, the KNTU CDRPM, an 8 actuated 6 DOF CDRPM, is considered as the case study of design. It is shown that weighting functions are able to provide a trade–off between various design criteria and give a total cost function for optimization. Finally, a combined numerical optimization algorithm is used to find the unique global optimum point. The result shows a significant enhancement in the performance characteristics of the KNTU CDRPM compared to that of the other CDRPMs. Since the proposed method is not restricted to any particular assumption on the objectives and design parameters, it can be used for optimal design of other manipulators.

References

[1] J. Merlet, Parallel Robots. Springer, 2006.

[2] T. Yoshikawa, "Manipulability of robotic mechanisms," The International Journal of Robotics Research, vol. 4, no. 2, pp. 3–9, 1985.

[3] F. Hao and J. Merlet, "Multi-criteria optimal design of parallel manipulators based on interval analysis," Mechanism and Machine Theory, vol. 40, no. 2, pp. 157–171, 2005.

[4] J. O. Kim, "Dexterity measures for design and control of manipulators," in IEEE Int. workshop on intelligent robots and systems, (Osaka, Japan), pp. 758–763, 1991.

[5] C. A. Klein and B. E. Blaho, "Dexterity measures for the design and control of kinematically redundant manipulators," International Journal of Robotics Research, vol. 6, pp. 72–83, Summer 1987.

[6] H. Asada, "A geometrical representation of manipulator dynamics and its application to arm design," Journal of dynamic systems, measurement, and control, vol. 105, no. 3, pp. 131–142, 1983.

[7] M. Hiller, S. Fang, S. Mielczarek, R. Vehoeven, and D. Franitza, "Design, analysis and realization of tendon-based parallel manipulators," Mechanism and Machine Theory, pp. 429–445, 2005.

[8] B. Dasgupta and T. Mruthyunjaya, "The Stewart Platform Manipulator: A Review," Mechanism and Machine Theory, vol. 35, no. 1, pp. 15–40, 2000.

[9] S. Tadokoro, M. H. Y. Murao, R. Murata, H. Kohkawa, and T. Matsushima, "A motion base with 6-dof by parallel cable drive architecture," IEEE/ASME Transactions on Mechatronics, vol. 7, pp. 115–123, June 2002.

[10] H. Li, C. Gosselin, M. Richard, and B. M. St-Onge, "Analytic form of the six-dimensional singularity locus of the general gough-stewart platform," ASME Journal of Mechanical Design, vol. 128, pp. 279–287, January 2006.

[11] L.L.Cone, "Skycam: an aerial robotic camera system," BYTE, pp. 122—132, Oct. 1985.

[12] H. D. Taghirad and M. Nahon, "Kinematic analysis of a macro-micro redundantly actuated parallel manipulator," Advanced Robotics, vol. 22, p. 657–687, July 2008.

[13] P. Bosscher, A. Riechel, and I. Ebert-Uphoff, "Wrench-Feasible Workspace Generation For Cable-Driven Robots," IEEE Transactions on Robotics, vol. 22, no. 5, pp. 890–902, 2006.

[14] M. Gouttefarde, J.-P. Merlet, and D. Daney, Advances in robot kinematics:mechanisms and motion, ch. Determination of the Wrench-Closure Workspace of 6-DOF Parallel Cable-Driven Mechanisms, pp. 315–322. Springer, 2006.

[15] S. Tadokoro and T. Matsushima, "A parallel cable-driven motion base for virtual acceleration," in Int. Conf. IROS, pp. 1700–1705, November 2001.

[16] M. Gouttefarde and C. Gosselin, "Analysis of the wrench-closure workspace of planar parallel cable-driven mechanisms," IEEE Transactions on Robotics, vol. 22, no. 3, pp. 434–445, 2006.

[17] J. Gott III and W. Colley, "Median statistics in polling," Mathematical and Computer Modelling, vol. 48, no. 9-10, pp. 1396–1408, 2008.

[18] L. Vanegas and A. Labib, "Application of new fuzzy-weighted average (nfwa) method to engineering design evaluation," International Journal of Production Research, vol. 39, no. 6, pp. 1147–1162, 2001.

[19] A. Zarif, M. M. Aref, and H. D. Taghirad, "Wrench feasible workspace analysis of cable-driven parallel manipulators using LMI approach." IEEE/ASME

International Conference on Advanced Intelligent Mechatronics (AIM), May 2009.

[20] K. Kozak, Q. Zhou, and J. Wang, "Static Analysis of Cable-Driven Manipulators with Non-Negligible Cable Mass," IEEE Transactions on Robotics, vol. 22, no. 3, pp. 425–433, 2006.

[21] S. Chang, J. Lee, and H. Yen, "Kinematic and compliance analysis for tendon-driven robotic mechanisms with flexible tendons," Mechanism and Machine Theory, vol. 40, no. 6, pp. 728–739, 2005.

[22] Y. Zhao, L. Wang, D. Chen, and L. Jiang, "Non-linear dynamic analysis of the two-dimensional simplified model of an elastic cable," Journal of Sound and Vibration, vol. 255, no. 1, pp. 43–59, 2002.

[23] P. Gholami, M. M. Aref, and H. D. Taghirad, "On the control of the KNTU CDRPM: A cable driven parallel manipulator," in IEEE/RSJ Int. Conf. IROS, pp. 2404–2409, September 2008.

[24] L. Yingjie, Z. Wenbai, and R. Gexue, "Feedback control of a cable-driven Gough-Stewart platform," IEEE Transactions on Robotics, vol. 22, no. 1, pp. 198–202, 2006.

[25] T. Bruckmann, L. Mikelsons, M. Hiller, and D. Schramm, "A new force calculation algotithm for tendon-based parallel manipulators," in IEEE Conf. on Advanced Intelligent Mechatronics, pp. 1–6, September 2007.

[26] C. M. Gosselin, "Optimum design of robotic manipulators using dexterity indices," Robotics and Autonomous Systems, vol. 9, no. 4, pp. 213–226, 1992.

[27] J. Merlet, "Jacobian, manipulability, condition number, and accuracy of parallel robots," Journal of Mechanical Design, vol. 128, pp. 199–206, 2006.

[28] S.-G. Kim and J. Ryu, "New dimensionally homogeneous jacobian matrix formulation by three end-effector points for optimal design of parallel manipulators," IEEE Transactions on Robotics and Automation, vol. 19, pp. 731–737, August 2003.

[29] C. Gosselin and J. Angeles, "A global performance index for the kinematic optimization of robotic manipulators," Journal of Mechanical Design, vol. 113, p. 220, 1991.

[30] M. Stock and K. Miller, "Optimal kinematic design of spatial parallel manipulators: application to linear Delta robot," Journal of Mechanical Design, vol. 125, p. 292, 2003.

[31] J.-P. Merlet and D. Daney, "Legs interference checking of parallel robots over a given workspace or trajectory," Proceedings of Int.Conference on Robotics and Automation, pp. 757–762, 2006.

[32] M. Aref and H. Taghirad, "Geometrical workspace analysis of a cable-driven redundant parallel manipulator: KNTU CDRPM," in IEEE Int.Conf. IROS, pp. 1958–1963, September 2008.

[33] D. Eberly, 3D game engine design : a practical approach to real-time computer graphics. Section 2.6 ,Morgan Kaufmann, 2001.

[34] T. Lee and M. Perng, "Analysis of simplified position and 5-dof total orientation workspaces of a hexapod mechanism," Mechanism and Machine Theory, vol. 42, pp. 1577–1600, 2007.

[35] Y. Hwang, J. Yoon, and J. Ryu, "The optimum design of a 6-dof parallel manipulator with large orientation workspace," SICE-ICASE Int. Joint Conference, 2006.

[36] A. Rao, P. Rao, and S. Saha, "Workspace and dexterity analyses of hexaslide machine tools," in IEEE International Conference on Robotics and Automation ICRA, vol. 3, 2003.

[37] C. Pham, S. Yeo, G. Yang, M. Kurbanhusen, and I. Chen, "Force-closure workspace analysis of cable-driven parallel mechanisms," Mechanism and Machine Theory, vol. 41, pp. 53–69, 2006.

[38] S. Bouchard, C. Gosselin, and B. Moore, "On the ability of a cable-driven robot to generate a prescribed set of wrenches," in Proc. of the ASME International Design Engineering Technical Conferences, Mechanics and Robotics Conference.

[39] X. Diao and O. Ma, "A method of verifying force–closure condition for general cable manipulators with seven cables," Mechanism and Machine Theory, vol. 42, pp. 1563–1576, 2007.

[40] M. Korayem, M. Bamdad, and M. Saadat, "Workspace analysis of cable-suspended robots with elastic cable," in IEEE International Conference on Robotics and Biomimetics, 2007. ROBIO 2007, pp. 1942–1947, 2007.

[41] R. Williams and P. Gallina, "Planar cable-direct-driven robots: design for wrench exertion," Journal of Intelligent and Robotic Systems, vol. 35, no. 2, pp. 203–219, 2002.

[42] E. Stump and V. Kumar, "Workspaces of cable-actuated parallel manipulators," Journal of Mechanical Design, vol. 128, p. 159, 2006.

[43] A. Fattah and S. Agrawal, "On the design of cable-suspended planar parallel robots," Journal of Mechanical Design, vol. 127, p. 1021, 2005.

[44] G. Barrette and C. Gosselin, "Determination of the dynamic workspace of cable-driven planar parallel mechanisms," Journal of Mechanical Design, vol. 127, p. 242, 2005.

[45] M. Hassan and A. Khajepour, "Optimization of Actuator Forces in Cable-Based Parallel Manipulators Using Convex Analysis," IEEE Transactions on Robotics, vol. 24, no. 3, pp. 736–740, 2008.

[46] C. Audet and J. Dennis, "R.(2003),"Analysis of generalized pattern searches,"," SIAM Journal on Optimization, vol. 13, pp. 889–903.

[47] M. Abramson, Pattern search algorithms for mixed variable general constrained optimization problems. PhD thesis, Ecole Polytechnique de Montreal, 2002.